



Chinese Pharmaceutical Association
Institute of Materia Medica, Chinese Academy of Medical Sciences

Acta Pharmaceutica Sinica B

www.elsevier.com/locate/apsb
www.sciencedirect.com



ORIGINAL ARTICLE

Fenofibrate-promoted hepatomegaly and liver regeneration are PPAR α -dependent and partially related to the YAP pathway



Shicheng Fan^{a,†}, Yue Gao^{b,†}, Pengfei Zhao^b, Guomin Xie^c,
Yanying Zhou^b, Xiao Yang^{a,e}, Xuan Li^a, Shuaishuai Zhang^a,
Frank J. Gonzalez^d, Aijuan Qu^c, Min Huang^b, Huichang Bi^{a,e,*}

^aNMPA Key Laboratory for Research and Evaluation of Drug Metabolism & Guangdong Provincial Key Laboratory of New Drug Screening & Guangdong-Hongkong-Macao Joint Laboratory for New Drug Screening, School of Pharmaceutical Sciences, Southern Medical University, Guangzhou 510515, China

^bGuangdong Provincial Key Laboratory of New Drug Design and Evaluation, School of Pharmaceutical Sciences, Sun Yat-sen University, Guangzhou 510006, China

^cDepartment of Physiology and Pathophysiology, School of Basic Medical Sciences, Capital Medical University, Beijing 100069, China

^dLaboratory of Metabolism, Center for Cancer Research, National Cancer Institute, National Institutes of Health, Bethesda, MD 20892, USA

^eThe State Key Laboratory of Chemical Oncogenomics, School of Chemical Biology and Biotechnology, Shenzhen Graduate School of Peking University, Shenzhen 518055, China

Received 20 November 2023; received in revised form 26 January 2024; accepted 3 March 2024

KEY WORDS

Fenofibrate;
PPAR α ;
Hepatomegaly;
Partial hepatectomy;
Liver regeneration;
YAP;
TEAD;
Ubiquitination

Abstract Fenofibrate, a peroxisome proliferator-activated receptor α (PPAR α) agonist, is widely prescribed for hyperlipidemia management. Recent studies also showed that it has therapeutic potential in various liver diseases. However, its effects on hepatomegaly and liver regeneration and the involved mechanisms remain unclear. Here, the study showed that fenofibrate significantly promoted liver enlargement and regeneration post-partial hepatectomy in mice, which was dependent on hepatocyte-expressed PPAR α . Yes-associated protein (YAP) is pivotal in manipulating liver growth and regeneration. We further identified that fenofibrate activated YAP signaling by suppressing its K48-linked ubiquitination, promoting its K63-linked ubiquitination, and enhancing the interaction and transcriptional activity of the YAP–TEAD complex. Pharmacological inhibition of YAP–TEAD interaction using verteporfin or

*Corresponding author.

E-mail address: bihchang@smu.edu.cn (Huichang Bi).

[†]These authors made equal contributions to the work.

Peer review under the responsibility of Chinese Pharmaceutical Association and Institute of Materia Medica, Chinese Academy of Medical Sciences.

<https://doi.org/10.1016/j.apsb.2024.03.030>

2211-3835 © 2024 The Authors. Published by Elsevier B.V. on behalf of Chinese Pharmaceutical Association and Institute of Materia Medica, Chinese Academy of Medical Sciences. This is an open access article under the CC BY-NC-ND license (<http://creativecommons.org/licenses/by-nc-nd/4.0/>).

suppression of YAP using AAV *Yap* shRNA in mice significantly attenuated fenofibrate-induced hepatomegaly. Other factors, such as MYC, KRT23, RAS, and RHOA, might also participate in fenofibrate-promoted hepatomegaly and liver regeneration. These studies demonstrate that fenofibrate-promoted liver enlargement and regeneration are PPAR α -dependent and partially through activating the YAP signaling, with clinical implications of fenofibrate as a novel therapeutic agent for promoting liver regeneration.

© 2024 The Authors. Published by Elsevier B.V. on behalf of Chinese Pharmaceutical Association and Institute of Materia Medica, Chinese Academy of Medical Sciences. This is an open access article under the CC BY-NC-ND license (<http://creativecommons.org/licenses/by-nc-nd/4.0/>).

1. Introduction

Partial hepatectomy (PHx) and liver transplantation are usually effective and the only available therapeutic means for several end-stage liver diseases¹. After PHx, the liver possesses a distinct ability for regeneration, ensuring restoration of liver size to 100% of its normal value². During liver regeneration following PHx, the remnant liver enlarges, accompanied by hepatocyte hypertrophy and enhanced hepatocyte proliferation, which is intrinsically a type of physiological/benign hepatomegaly³. Ensuring attainment of the minimal liver size is important for good outcomes, as an undersized remnant liver post-surgery might lead to perioperative liver failure and even death⁴. Despite significant advancements achieved in surgical methods, effective clinical medications to maximize liver regeneration are lacking⁵. Thus, it is of great value to find new medications for inducing benign hepatomegaly and promoting liver regeneration after PHx.

The process of liver regeneration is regulated by an intricate network of signaling pathways⁶. Various signaling, such as cytokines and growth factors, play essential roles in regulating liver regeneration^{7,8}. Yes-associated protein (YAP), the core factor of the Hippo pathway, was reported to manipulate liver homeostasis. YAP typically undergoes phosphorylation through the mammalian STE20-like protein kinase 1/2 (MST1/2)-large tumor suppressor 1/2 (LATS1/2), leading to its sequestration in the cytoplasm. When YAP is activated, it is unphosphorylated and translocates into the nucleus, then interacts with TEA domain transcription factor (TEAD) to activate downstream targets⁹. Activation of YAP in mice was found to induce significant hepatomegaly, leading to a 4.1-fold increase in liver size¹⁰. In addition, previous studies showed that YAP activation increases cell size and promotes cell proliferation through distinct mechanisms¹¹. Moreover, YAP was found to orchestrate liver regeneration. Inhibition of MST1/2, which resulted in YAP activation, improved liver regeneration post-PHx¹². Deletion of *Yap* in hepatocytes inhibited epithelial-to-mesenchymal transition after PHx, leading to impairment of liver regeneration¹³.

Previous studies have demonstrated that several small-molecule drugs and FDA-approved medications can promote hepatomegaly and liver regeneration. For example, Zhang et al.¹⁴ discovered that inhibiting 15-hydroxyprostaglandin dehydrogenase with SW033291 enhances liver regeneration following PHx in mice. MST1/2 inhibitor XMU-MP-1, developed by Fan et al.¹⁵, could activate the YAP pathway and promote liver regeneration post-PHx. Moreover, bardoxolone methyl (CDDO-Me), a potent Nrf2 activator, has shown significant efficacy in liver volume and function recovery in PHx models, primarily through promoting hepatocyte hypertrophy and proliferation, and reducing

inflammatory responses¹⁶. Activation of constitutive androstane receptor (CAR) through agonists like TCPOBOP (murine) or CITCO (human) has been found to provoke hepatomegaly and liver regeneration in mouse models^{17,18}. Our studies revealed that the pregnane X receptor (PXR) activators PCN and rifampicin promote liver regeneration through YAP signaling activation¹⁹. Schisandrol B has been shown hepatomegaly-inducing effects by activating PXR and YAP²⁰. Carbamazepine, commonly used for seizure control and mood stabilization, has shown hepatoproliferative effects *via* mTOR signaling activation post-PHx in mice²¹. Dexmedetomidine pretreatment aids in liver regeneration and function recovery by inhibiting NLRP3 inflammasome activation²². Our studies also revealed that high-dose dexamethasone treatment induces hepatomegaly and hepatocyte enlargement in mice, mediated by the PXR–YAP activation and lipid accumulation²³. A high dose of mifepristone, a synthetic antiprogestogen, was found to induce hepatomegaly in mice by activating PXR and YAP pathway²⁴.

Fenofibrate is widely prescribed for hyperlipidemia management²⁵. However, the pharmacological effects of fenofibrate are not limited to lipid regulation. It plays a significant role in modulating hepatic glucose and bile acid homeostasis while impacting oxidative stress and inflammatory responses within the liver²⁶. These multifaceted effects of fenofibrate underscore its therapeutic potential in various liver diseases. For instance, fenofibrate has demonstrated efficacy in ameliorating metabolic syndrome in non-alcoholic fatty liver disease (NAFLD) patients^{27,28}. Additionally, it has been utilized in treating chronic cholestatic liver disease patients unresponsive to ursodeoxycholic acid (UDCA) monotherapy in several clinical trials^{29,30}. Furthermore, in animal models, fenofibrate has shown promising results in treating liver fibrosis and drug-induced liver injury^{31,32}. Fenofibrate has been identified as a classical agonist of peroxisome proliferator-activated receptor α (PPAR α), a critical modulator of lipid and energy homeostasis³³. We recently found that selective PPAR α activator WY-14643 induced liver growth and promoted liver regeneration by interacting with YAP signaling pathway³⁴. Fenofibrate has been observed to induce hepatomegaly; however, the precise mechanisms underlying this phenomenon remain to be fully elucidated^{35,36}. Moreover, the effects of fenofibrate on liver regeneration post-PHx and the role of YAP in this context remain unclear.

Here, we found that fenofibrate promoted hepatomegaly and liver regeneration, which was PPAR α -dependent, and PPAR α expressed in hepatocytes played the dominant role in these processes. Fenofibrate treatment activated YAP signaling by regulating the ubiquitination of YAP and YAP–TEAD transcriptional activity. Suppression of the YAP pathway using

YAP–TEAD interaction inhibitor or AAV *Yap* shRNA system significantly repressed fenofibrate-induced liver enlargement. Finally, MYC proto-oncogene (MYC), keratin 23 (KRT23), ras homolog family member A (RHOA), and RAS proto-oncogene (RAS) were also found to be associated with the fenofibrate-induced hepatic proliferative response.

2. Materials and methods

2.1. Animals

Wild-type C57BL/6 mice (male, 8–9 weeks old) were purchased from Guangdong Medical Laboratory Animal Center (Foshan, China). *Ppara*^{fl/fl} and hepatocyte-specific *Ppara*-deficient (*Ppara*^{ΔHep}) mice were generated as previously described³⁷. Wild-type mice were intravenously injected with AAV-Control-EGFP or AAV-*Yap*-shRNA-EGFP (1.1×10^{11} genome copies per mouse, Hanbio Co., Ltd., Shanghai, China) to establish the *Yap* knock-down mouse models.

Wild-type mice were intragastrically injected with corn oil (Aladdin, Cat# C116025, Shanghai, China) or with 25, 50, or 100 mg/kg/day fenofibrate (APEX BIO Technology LLC, Cat# B1943, USA) for 10 days. *Ppara*^{fl/fl} and *Ppara*^{ΔHep} mice were intragastrically injected with corn oil or 50 mg/kg/day fenofibrate for 10 days. Wild-type mice were intragastrically injected with corn oil or 50 mg/kg/day fenofibrate following PHx, and tissue and serum samples were collected 2 and 5 days after the surgery. *Ppara*^{fl/fl} and *Ppara*^{ΔHep} mice were intragastrically injected with corn oil or 50 mg/kg/day fenofibrate following PHx, and tissue and serum samples were collected 2 days after the surgery. Wild-type mice were intraperitoneally injected with 100 mg/kg/day verteporfin (CSNpharm, Cat# CSN12195, USA) or intragastrically injected with 50 mg/kg/day fenofibrate for 10 days. Wild-type mice were intravenously injected with AAV-Control-EGFP or AAV-*Yap*-shRNA-EGFP. After 4 weeks for YAP interference, the mice were intragastrically injected with 50 mg/kg/day fenofibrate for 10 days. Serum and liver tissue samples were collected, snap-frozen in liquid nitrogen, and stored at -80°C for further use. A portion of the liver was immediately fixed with 10% formalin buffer for further histological analysis. All animal experiments and protocols were approved by the Institutional Animal Care and Use Committee of Sun Yat-sen University (Guangzhou, China, Approve No. SYSU-IACUC-2022000885).

2.2. Histological and biochemical assessments

As described in our previous publication¹⁹, liver samples were collected, fixed with formalin, and embedded in paraffin. Paraffin-embedded sections were further subjected to staining with hematoxylin and eosin (H&E), an anti- β -catenin antibody (BD Biosciences, Cat# 610153, San Jose, CA, USA), and an anti-KI67 antibody (Abcam, Cat# ab15580, Cambridge, UK). The stained liver sections were observed and analyzed with an Olympus BX41 microscope system. As previously described¹⁹, for quantification of CTNBN1 staining, ImageJ software (National Institutes of Health, Bethesda, USA) was employed to measure the visual field of the liver sections and calculate the average hepatocyte size. For KI67 staining, the KI67⁺ cells were counted, and the percentage of KI67⁺ cells in the whole section was then calculated.

The levels of serum alanine aminotransferase (ALT), aspartate transaminase (AST), and alkaline phosphatase (ALP) were measured by commercially available kits (Nanjing Jiancheng

Bioengineering Institute, Nanjing, China) according to the manufacturer's instructions.

2.3. Quantitative real-time PCR analysis

As previously reported¹⁷, total RNA from liver samples was extracted, and cDNA was obtained by reverse transcription of 1 μg of RNA. Real-time PCR was conducted on a Biosystems 7500 Real-Time PCR System. The $\Delta\Delta\text{Ct}$ method was employed to calculate the relative mRNA levels of genes of interest.

2.4. Western blot analysis

As previously published¹⁷, the protein was extracted, and the concentration was then determined by a BCA Protein Assay Kit (Thermo Scientific, Rockford, IL, USA). Proteins in samples were separated by SDS-PAGE and were then transferred onto polyvinylidene fluoride membranes. After being blocked with 5% nonfat milk, the membranes were incubated with different antibodies overnight. Incubation of secondary antibodies was performed at room temperature. An ECL Detection Kit (Millipore, Darmstadt, Germany) and chemiluminescence detection systems (Bio-Rad, CA, USA) were employed to develop the blots and identify proteins.

2.5. Dual-luciferase reporter assay

The YAP luciferase reporter construct $8 \times \text{GTIC}$ (#34615) was purchased from Addgene. To investigate the effect of fenofibrate on YAP transcriptional activity, HepG2 cells were transiently co-transfected with the Flag-YAP, $8 \times \text{GTIC}$, and *Renilla* plasmids. Cells were then treated with 50 $\mu\text{mol/L}$ fenofibrate or vehicle for 24 h. Luciferase activity was measured by a Dual-Luciferase Reporter Assay System Kit (Promega, San Luis Obispo, CA, USA).

2.6. Co-immunoprecipitation (co-IP) assay

For the experiment testing the effect of fenofibrate on YAP ubiquitination, HepG2 cells (ATCC, Cat# HB-8065, RRID: CVCL_0027, VA, USA) were cotransfected with the Flag-YAP and HA-Ub/HA-Ub-K48/HA-Ub-K63 plasmids and were then treated with fenofibrate. The cells were treated with 20 $\mu\text{mol/L}$ MG132 for 6 h before harvesting. Co-IP was performed with a Thermo Scientific Pierce co-IP kit (Thermo Scientific, Rockford, IL, USA). Samples were analyzed by Western blot.

2.7. Statistical analysis

Data are presented as the mean \pm standard deviation (mean \pm SD) values. Data were analyzed using SPSS (version 27.0) and GraphPad Prism (version 10.1.2) software. The sample size/number of experiments was set before data were obtained. Statistical significance was determined using unpaired two-tailed Student's *t*-test between two groups and one-way ANOVA with Dunnett's *post hoc* test for multi-group comparisons. *P* values < 0.05 were considered to indicate significant differences. The *P* values are noted in each figure legend and indicated as exact values or */**/***/****, which indicates $P < 0.05/0.01/0.001/0.0001$, respectively, versus the Control. The statistical details for each experiment are indicated in the figure legend.

Detailed information on antibodies used for Western blot and IP analyses and real-time PCR primer sequences is available within the Supporting Information.

3. Results

3.1. Fenofibrate-induced hepatomegaly is PPAR α -dependent

To assess the impact of fenofibrate on liver size, male C57BL/6 mice were administered different dosages of fenofibrate (Fig. 1A). As

shown in Fig. 1B, upon fenofibrate administration, the liver-to-body weight ratios exhibited an elevation in contrast to the vehicle-treated group. Assessment of liver morphology also revealed obvious hepatomegaly after fenofibrate administration (Fig. 1C). No observable liver damage was found by H&E staining after fenofibrate treatment (Fig. 1D). The levels of biochemical indexes, including ALT, AST, and ALP were not obviously altered upon fenofibrate treatment (Supporting Information Fig. S1A). To determine whether fenofibrate-induced hepatomegaly is related to inflammation response, we detected the mRNA levels of inflammatory factors

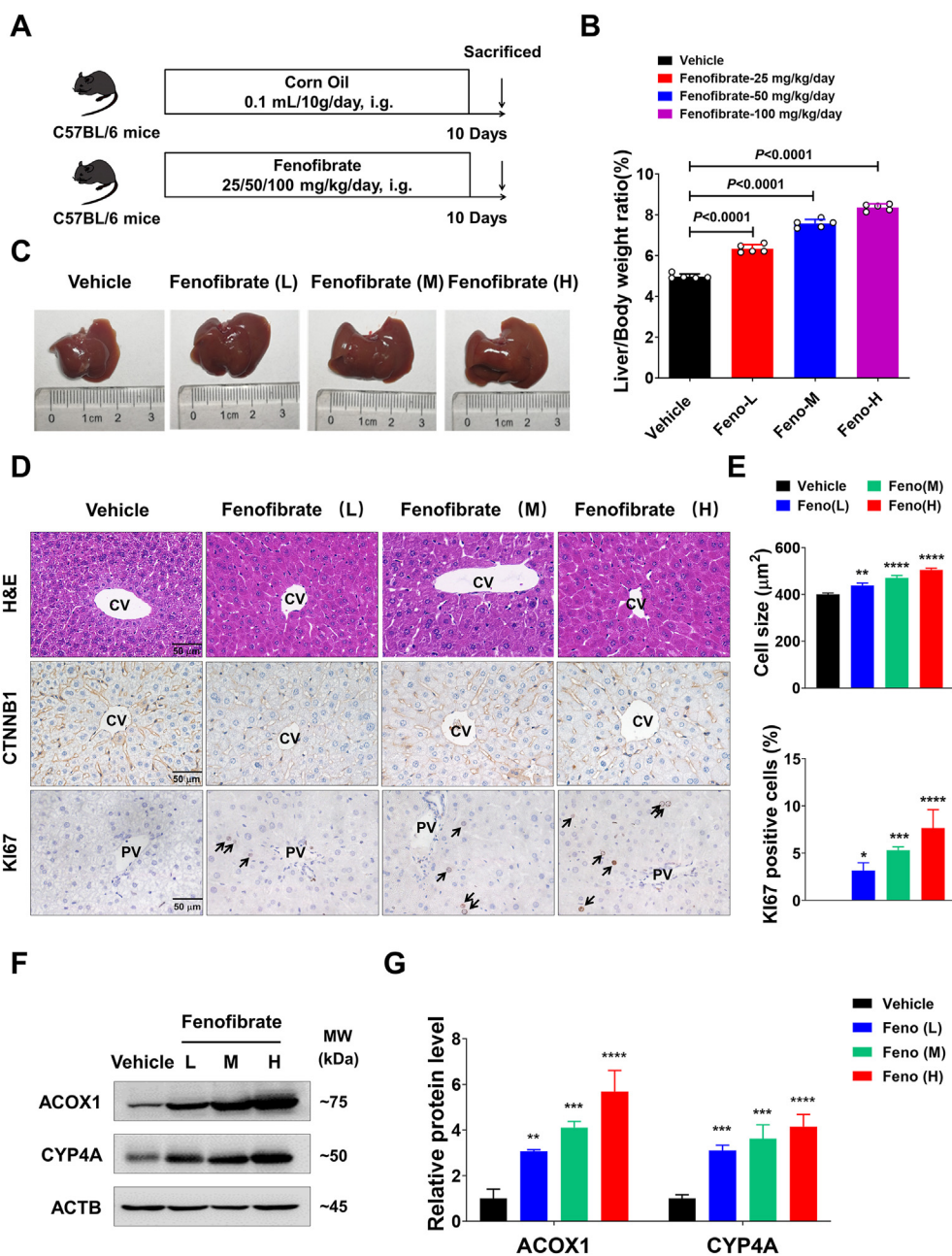


Figure 1 Fenofibrate induced liver enlargement in C57BL/6 mice. (A) Experimental procedure in C57BL/6 mice. (B) Ratios of liver weight to body weight ($n = 5$). (C) Photographs of mouse livers in each group. (D) H&E, CTNNB1, and KI67 staining. (E) Quantitative analysis of cellular size and determination of KI67⁺ cell proportion ($n = 3$). (F) Western blot analysis related to the PPAR α downstream targets, specifically ACOX1 and CYP4A. (G) Quantification of ACOX1 and CYP4A expression ($n = 3$). Data are depicted as the mean \pm SD values; */**/***/**** indicates $P < 0.05/0.01/0.001/0.0001$, respectively, versus the Control. Scale bar = 50 μm . Feno (L), Feno (M), or Feno (H) indicates the low, medium, and high (25/50/100 mg/kg/day) dosage of the fenofibrate.

interleukin 6 (*Il-6*) and tumor necrosis factor alpha (*Tnfa*) in the liver of mice treated with fenofibrate (Supporting Information Fig. S2A). The results showed that fenofibrate did not significantly alter the hepatic mRNA levels of *Il-6* and *Tnfa*. CTNNB1 immunostaining was employed to analyze hepatocyte size, revealing a notable enlargement of cell size neighboring the central vein (CV) area following fenofibrate treatment (Fig. 1D and E). However, the hepatocellular size surrounding the portal vein (PV) area between the two groups was not changed (Supporting Information Fig. S3A). KI67 staining was performed to determine the number of proliferating hepatocytes. Fenofibrate treatment dramatically elevated the proportion of KI67⁺ cells adjacent to the PV area (Fig. 1D and E), indicating that fenofibrate promoted hepatocyte proliferation. However, no observable KI67⁺ cells existed around the CV area in either the vehicle or fenofibrate-treated groups (Supporting Information Fig. S4A).

Fenofibrate has been reported to be a PPAR α agonist, and PPAR α activation can promote hepatocyte proliferation and hepatomegaly^{33,34}. Thus, we measured the expression of the PPAR α downstream proteins. Fenofibrate treatment markedly upregulated the expression of acyl-CoA oxidase 1 (ACOX1) and cytochrome P450 family 4 subfamily A (CYP4A) (Fig. 1F and G), indicating that PPAR α was activated upon fenofibrate treatment. Studies have shown that hepatocyte-expressed PPAR α , not non-parenchymal cell-expressed PPAR α , is the major contributor to agonist-induced hepatocyte proliferation³⁷. Thus, we used the *Ppara* ^{Δ Hep} mouse model to assess the role of hepatocyte PPAR α in fenofibrate-induced hepatomegaly. Hepatic mRNA and protein expression of PPAR α were diminished in *Ppara* ^{Δ Hep} mice compared to those of *Ppara*^{fl/fl} mice (Supporting Information Fig. S5A and S5B). Fenofibrate significantly increased the liver-to-body weight ratios of *Ppara*^{fl/fl} mice but exerted no obvious effect on those of *Ppara* ^{Δ Hep} mice (Fig. 2A–C). H&E staining, together with measurement of biochemical indexes, indicated no apparent liver damage after fenofibrate treatment (Fig. 2D and E). Hepatic mRNA levels of *Il-6* and *Tnfa* in *Ppara*^{fl/fl} and *Ppara* ^{Δ Hep} mice remained statistically unchanged upon fenofibrate treatment (Fig. S2B). Hepatocytes surrounding the CV area displayed enlargement, while the count of KI67⁺ cells surrounding the PV area exhibited a marked rise after fenofibrate administration in *Ppara*^{fl/fl} mice. In contrast, fenofibrate did not induce hepatocyte hypertrophy and proliferation in *Ppara* ^{Δ Hep} mice (Fig. 2E and F and Supporting Figs. S3B and S4B). Additionally, ACOX1 and CYP4A were upregulated by fenofibrate treatment in *Ppara*^{fl/fl} mice, although their expression remained unchanged in fenofibrate-treated *Ppara* ^{Δ Hep} mice (Supporting Information Fig. S6A). These results demonstrated that PPAR α expressed in hepatocytes plays a dominant role in fenofibrate-induced liver enlargement.

3.2. Fenofibrate promotes liver regeneration through activation of PPAR α

To further investigate whether fenofibrate can promote PHx-induced liver regeneration, 2/3 hepatectomy was performed, and the hepatectomized mice were then administered fenofibrate (Supporting Information Fig. S7A). Compared with those in the vehicle group, the liver size exhibited a significant elevation by fenofibrate administration (Fig. S7B and S7C). Fenofibrate did not significantly alter the levels of serum indexes despite inducing a decrease in the ALP level 2 days after surgery (Fig. S7D). H&E staining revealed an absence of evident hepatic impairment after

fenofibrate treatment (Fig. S7E). CTNNB1 and KI67 staining depicted hepatocyte hypertrophy within the CV area and a substantial increase in the count of KI67⁺ cells surrounding the PV area in response to fenofibrate treatment (Figs. S7E, S7F, S3C and S4C). Moreover, fenofibrate induced the expression of the PPAR α downstream protein ACOX1 and CYP4A post-PHx (Fig. S6B), indicating PPAR α was activated during fenofibrate-promoted liver regeneration. To determine the role of hepatocyte PPAR α in fenofibrate-promoted liver regeneration, we performed 2/3 PHx on *Ppara*^{fl/fl} and *Ppara* ^{Δ Hep} mice and then treated the mice with fenofibrate for 2 days (Fig. 3A). Hepatic mRNA and protein expression of PPAR α were diminished in *Ppara* ^{Δ Hep} mice compared to those of *Ppara*^{fl/fl} mice (Supporting Information Fig. S5C and S5D). Fenofibrate promoted the increase of liver size and liver/body weight ratio in *Ppara*^{fl/fl} mice, which was abolished in *Ppara* ^{Δ Hep} mice (Fig. 3B and C). H&E staining and measurement of biochemical indexes suggested that no obvious liver injury occurred (Fig. 3D and E). Hepatocyte enlargement around the CV area and enhanced hepatocyte proliferation around the PV area were observed during fenofibrate-promoted liver regeneration in *Ppara*^{fl/fl} mice, which was absent in *Ppara* ^{Δ Hep} mice (Fig. 3E, F, and Figs. S3D and S4D). ACOX1 and CYP4A were upregulated by fenofibrate treatment in *Ppara*^{fl/fl} mice following PHx. However, their expression remained unchanged in fenofibrate-treated *Ppara* ^{Δ Hep} mice following PHx (Fig. S6C). Additionally, fenofibrate did not significantly alter the hepatic mRNA levels of *Il-6* and *Tnfa* post-PHx (Fig. S2C and S2D). These results suggested that fenofibrate accelerated liver weight restoration and promoted hepatocyte hypertrophy and proliferation in a hepatocyte PPAR α -dependent manner, which could potentially aid in the facilitation of liver regeneration after the surgery.

3.3. Fenofibrate regulates YAP ubiquitination and promotes YAP–TEAD activity

The YAP signaling cascade is pivotal in governing liver growth and liver regeneration⁹. Our earlier investigation discovered that the PPAR α activation, prompted by WY-14643, stimulated hepatomegaly and liver regeneration via the YAP–TEAD pathway³⁴. YAP is a transcriptional co-activator that mainly interacts with TEAD transcription factors to promote the expression of downstream targets such as connective tissue growth factor (CTGF), cysteine rich angiogenic inducer 61 (CYR61), and ankyrin repeat domain 1 (ANKRD1) (Fig. 4A). To explore whether the YAP is implicated in fenofibrate-induced liver enlargement and liver regeneration, we measured the expression of YAP and its downstream targets in all mouse models. Fenofibrate treatment significantly upregulated the mRNA levels of *Ctgf*, *Cyr61*, and *Ankrd1* (Fig. 4B and C, and Supporting Information Fig. S8A and S8B), indicating the activation of the YAP transcriptional program. We subsequently isolated the cytoplasmic and nuclear protein fractions. The protein levels of ACTB and LMNB1 were detected in the cytoplasmic and nuclear extracts, suggesting the effective separation of cytoplasmic and nuclear components (Supporting Information Fig. S9A–S9D). In C57BL/6, *Ppara*^{fl/fl} mice, or these mice following PHx, administration of fenofibrate resulted in elevated expression of total YAP, nuclear YAP, and downstream targets of YAP. Conversely, the expression of cytoplasmic phosphorylated (p)-YAP was diminished (Fig. 4D–G and Supporting Information Fig. S10A–S10D). These alterations collectively suggested the activation of the YAP signaling in

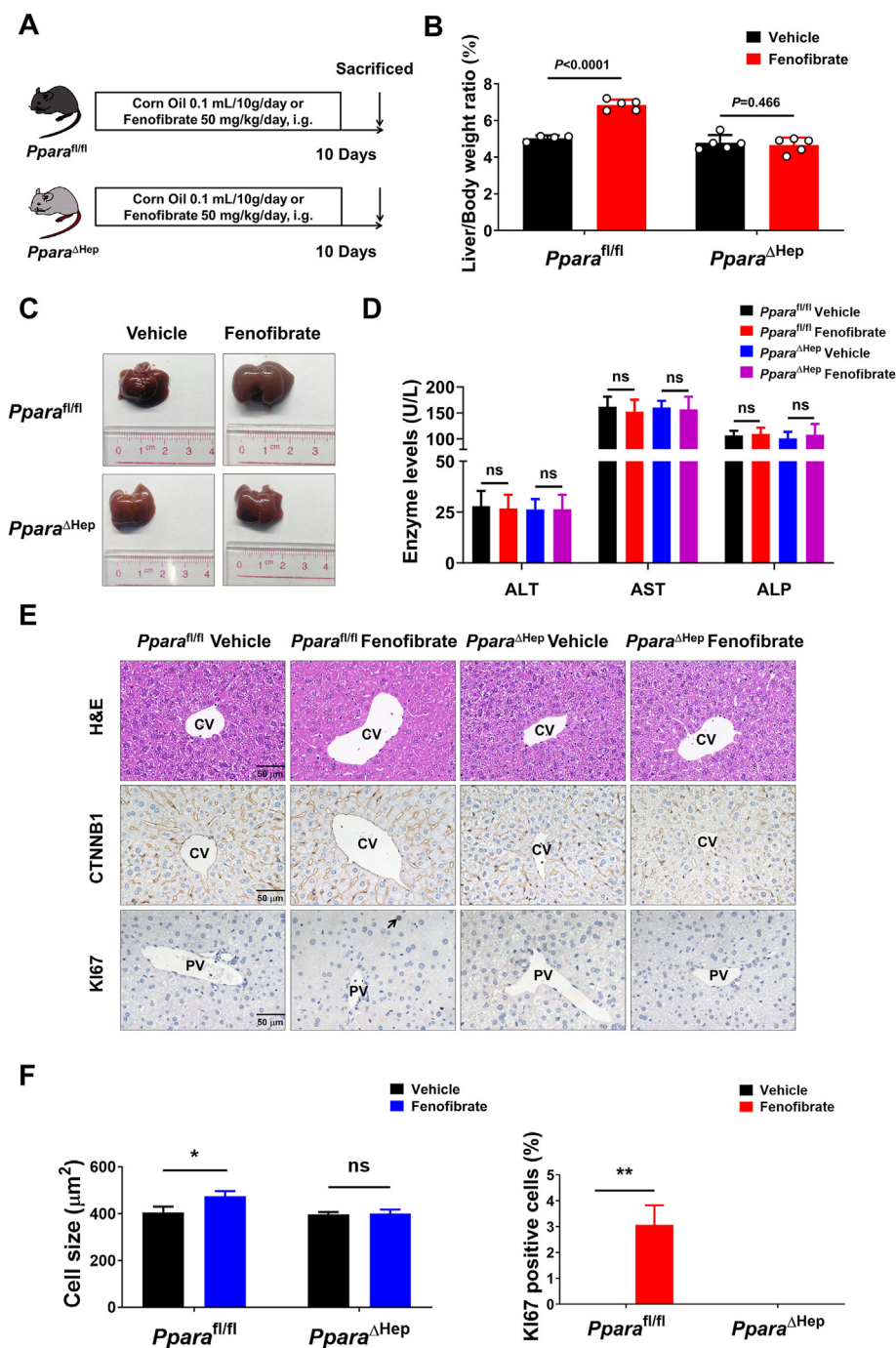


Figure 2 Hepatocyte-specific *Ppara* knockout abolished fenofibrate-induced hepatomegaly. (A) Experimental procedure in *Ppara*^{fl/fl} and *Ppara*^{ΔHep} mice. (B) Ratios of liver weight to body weight ($n = 4-5$). (C) Photographs of mouse livers in each group. (D) The levels of serum indexes ($n = 4-5$). (E) H&E, CTNNB1, and Ki67 staining. (F) Quantitative analysis of cellular size and determination of Ki67⁺ cell proportion ($n = 3$). Data are depicted as the mean \pm SD values; */** indicates $P < 0.05/0.01$, ns indicates not significant, versus the Control. Scale bar = 50 μ m.

these models. Cyclin proteins such as cyclin A1 (CCNA1) and cyclin D1 (CCND1) were also elevated in fenofibrate-treated wild-type, *Ppara*^{fl/fl}, and PHx mice (Supporting Information Fig. S11A–S11D). However, the levels of YAP signaling pathway proteins and cell cycle-related proteins were not significantly altered upon fenofibrate administration in *Ppara*^{ΔHep} mice (Fig. 4D–G and Fig. S11B and S11D),

suggesting that ablation of hepatocyte PPAR α impairs YAP activation induced by fenofibrate.

Apart from phosphorylation, the activity of YAP is additionally regulated by the process of ubiquitination, which is closely involved in its transcriptional activity³⁸. As shown in Fig. 4H, the levels of ubiquitinated YAP were decreased after fenofibrate treatment. It has been demonstrated that YAP undergoes

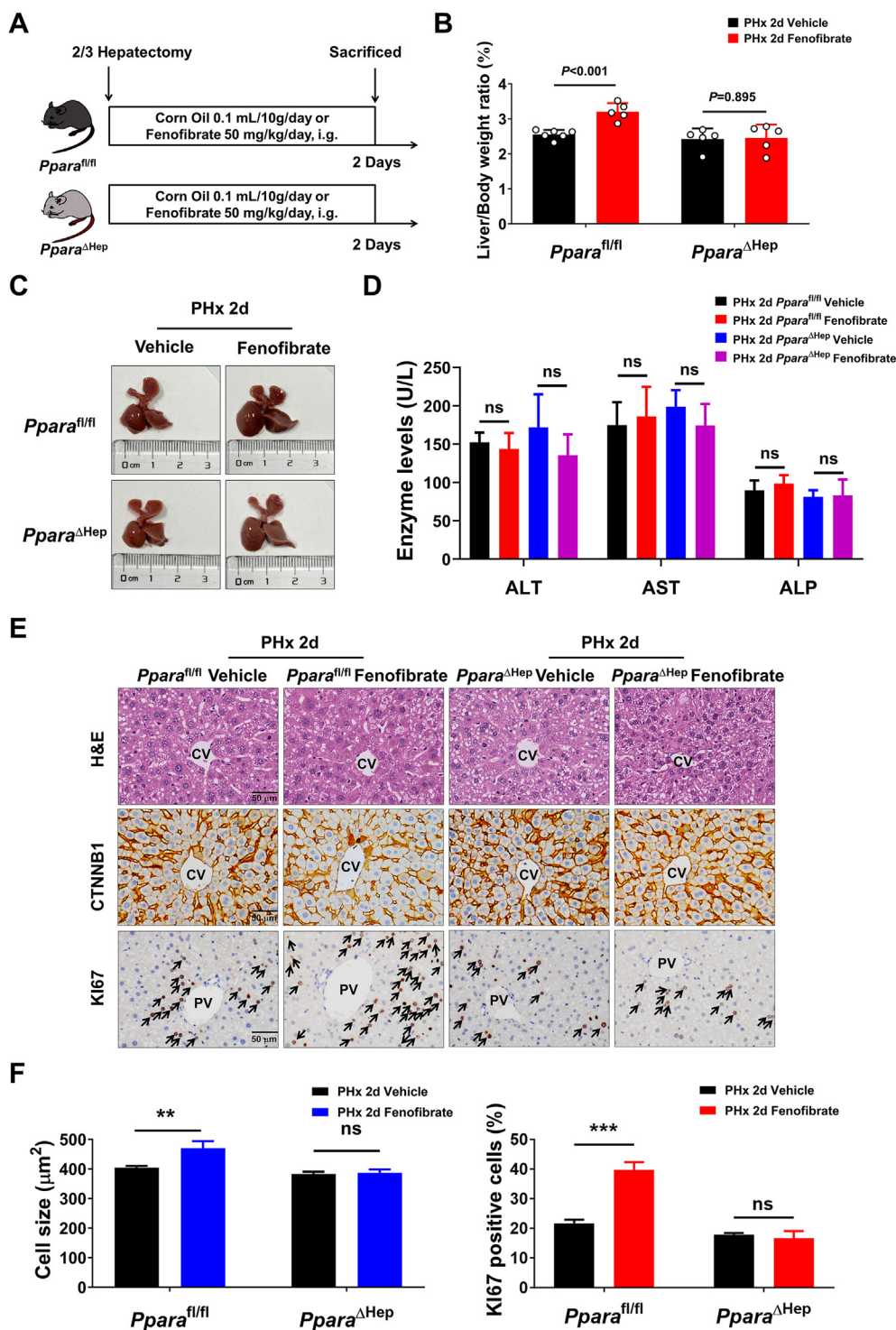


Figure 3 Fenofibrate promoted liver regeneration, but hepatocyte-specific *Ppara* knockout abolished fenofibrate-promoted liver regeneration following PHx. (A) Experimental procedure in *Ppara*^{fl/fl} and *Ppara*^{ΔHep} mice following PHx. (B) Ratios of liver weight to body weight ($n = 5-6$). (C) Photographs of mouse livers in each group. (D) The levels of serum indexes ($n = 5-6$). (E) H&E, CTNNB1, and KI67 staining. (F) Quantitative analysis of cellular size and determination of KI67⁺ cell proportion ($n = 3$). Data are depicted as the mean \pm SD values; **/** indicates $P < 0.01/0.001$, ns indicates not significant, versus the Control. Scale bar = 50 μ m.

degradation through K48-linked ubiquitination. In contrast, K63-linked ubiquitination of YAP enhances its transcriptional activity and stimulates growth-promoting effects^{39,40}. Then, we examined the effects of fenofibrate on YAP in the context of these two common ubiquitination modes. After fenofibrate treatment, K48-

linked YAP polyubiquitination was downregulated, while K63-linked YAP polyubiquitination was upregulated (Fig. 4I and J), suggesting that fenofibrate promotes the activity of YAP by suppressing its K48-linked ubiquitination and enhancing its K63-linked ubiquitination.

YAP regulates target genes by interacting with TEAD⁴¹; thus, the interaction and transcriptional activity of YAP–TEAD are essential for YAP-mediated gene regulation and proliferative responses. We next investigated whether fenofibrate can regulate the interaction and transcriptional activity of YAP–TEAD. Co-IP experiments revealed that the interaction of YAP and TEAD was obviously enhanced upon fenofibrate treatment (Fig. 4K). Moreover, as shown in Fig. 4L, fenofibrate substantially augmented the activity of the YAP–TEAD luciferase reporter ($8 \times$ GTIIC). These findings suggested that fenofibrate promoted the interaction between YAP and TEAD, thereby boosting its transcriptional activity.

3.4. The interaction between YAP and TEAD contributes to fenofibrate-induced hepatomegaly

When the upstream regulators in the Hippo pathway are inhibited, YAP undergoes dephosphorylation and subsequently relocates to the nucleus. As a transcription co-activator, the engagement with TEAD within the nucleus becomes crucial for facilitating YAP's transcriptional activity⁴¹. Verteporfin, a compound that hinders the interaction between YAP and TEAD, was employed to explore the impact of YAP–TEAD interaction on the liver enlargement induced by fenofibrate (Fig. 5A). The C57BL/6 mice were administered with verteporfin and/or fenofibrate for 10 days (Fig. 5B). A co-IP experiment was performed on hepatic proteins extracted from the livers of mice treated with either vehicle or verteporfin. The results showed that there exists protein–protein interaction between YAP and TEAD, and verteporfin treatment could disrupt this interaction (Fig. 5C). The result showed that verteporfin significantly mitigated fenofibrate-induced liver enlargement (Fig. 5D and E). The detection of ALT, AST, and ALP together with H&E staining indicated that either verteporfin or fenofibrate treatment did not induce obvious liver injury (Fig. 5F, and Fig. S1B). Verteporfin or fenofibrate treatment did not significantly alter the hepatic mRNA levels of *Il-6* and *Tnfa* (Fig. S2E). The CTNNB1 and KI67 staining showed that fenofibrate treatment promoted hepatocellular hypertrophy in the vicinity of the CV area and increased hepatocellular proliferation surrounding the PV area, which was significantly attenuated by verteporfin administration (Fig. 5F and G). Either verteporfin or fenofibrate treatment exerted no obvious effect on the hepatocellular size surrounding the PV area and failed to induce KI67⁺ cells in the vicinity of the CV area in all groups (Fig. S3E and S4E). We further detected the mRNA levels of *Ctgf*, *Cyr61*, and *Ankrd1* in the verteporfin-treated mice. The results showed that fenofibrate upregulated the mRNA levels of YAP downstream targets, which was compromised by verteporfin treatment (Fig. S8C). Moreover, the induction effects of fenofibrate on CTGF, ANKRD1, as well as cyclin proteins CCND1 and cyclin E1 (CCNE1) were mitigated upon the inhibition of YAP–TEAD interaction (Supporting Information Fig. S12A and S12B). Fenofibrate induced the protein expression of ACOX1 and CYP4A in the Control group and verteporfin-treated group (Fig. S6D), suggesting the agonistic effect of fenofibrate on PPAR α is not dependent on YAP–TEAD interaction. These findings suggest that the YAP–TEAD interaction is essential for hepatomegaly induced by fenofibrate.

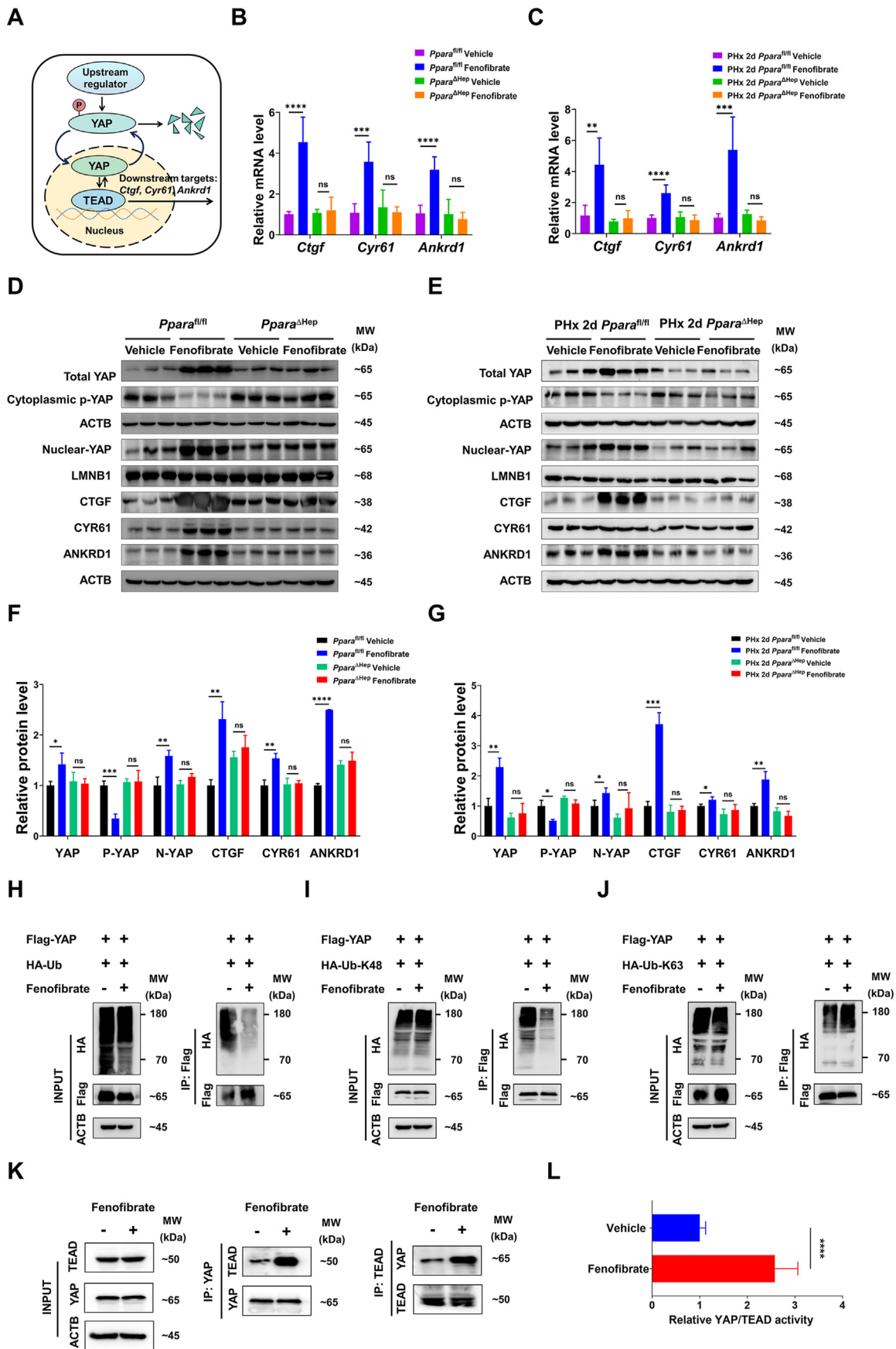
3.5. Fenofibrate-induced hepatomegaly is partially related to YAP

To further investigate the involvement of YAP in the hepatomegaly induced by fenofibrate, the AAV *Yap* shRNA mouse model

was employed and treated with fenofibrate (Fig. 6A). As shown in Fig. 6B and C, hepatic YAP protein expression was significantly decreased by AAV *Yap* shRNA transduction. Fenofibrate induced significant hepatomegaly in both AAV Control mice and AAV *Yap* shRNA mice. However, the mean ratio of liver-to-body weight in AAV *Yap* shRNA-treated mice was lower than that in AAV Control mice (6.45% versus 8.56%, $P < 0.0001$), demonstrating that YAP disruption suppresses fenofibrate-induced liver enlargement. Moreover, notably, a slight reduction in liver size was observed in vehicle-treated AAV *Yap* shRNA mice, suggesting the involvement of YAP in maintaining a normal liver size (Fig. 6D and E). Analysis of serum indexes and H&E staining showed no apparent liver damage following fenofibrate treatment in the AAV-treated models (Fig. 6F and Fig. S1C). Fenofibrate treatment did not significantly alter the hepatic mRNA levels of *Il-6* and *Tnfa* (Fig. S2F). The effect of YAP disruption on fenofibrate-promoted hepatocyte hypertrophy and proliferation was then examined. Hepatocytes in the vicinity of the CV area were enlarged and the count of KI67⁺ cells surrounding the PV area was increased in both groups. However, mice with hepatic disruption of YAP showed less hepatocyte enlargement and proliferation than their counterparts in the AAV Control group (Fig. 6F and G). In contrast, fenofibrate treatment did not obviously affect the size of PV zone-surrounded hepatocytes, and there was no observed rise in the count of KI67⁺ cells within the CV area in any group (Figs. S3F and S4F). Moreover, fenofibrate treatment upregulated the mRNA and protein expression of YAP targets in AAV-Control mice but did not significantly affect those in AAV *Yap* shRNA mice (Figs. S8D and S12C). CCND1 and CCNE1 were upregulated by fenofibrate in the Control group, but their expression remained unchanged when YAP was disrupted. In contrast, CCNA1 still showed a pronounced upregulation after fenofibrate treatment when hepatic YAP was knocked down (Fig. S12D). Fenofibrate induced the protein expression of ACOX1 and CYP4A in both groups (Fig. S6E), suggesting the PPAR α activation induced by fenofibrate is not dependent on YAP. These results demonstrated that hepatic YAP disruption attenuated fenofibrate-induced hepatomegaly, hepatocyte enlargement, and hepatocyte proliferation in mice.

3.6. Other factors are associated with fenofibrate-promoted hepatomegaly and liver regeneration

Knockdown of *Yap* or pharmacological inhibition of YAP–TEAD attenuated but not totally abolished fenofibrate-induced hepatomegaly. We hypothesized that there might be other factors that participated in fenofibrate-promoted liver enlargement and liver regeneration. Thus, we further checked the mRNA and protein expression of *Myc*, *Krt23*, *Kras*, and *Rhoa*, which were previously implicated in PPAR α -induced hepatomegaly and liver regeneration^{42–44}. *Myc*, *Krt23*, *Kras*, and *Rhoa* were upregulated after fenofibrate treatment in both the Control and *Yap* knockdown model (Fig. 7A). Fenofibrate treatment significantly upregulated the protein expression of MYC, KRT23, and KRAS in both groups (Fig. 7B and C). The protein level of RHOA remained statistically unchanged but showed an increasing trend upon fenofibrate treatment in AAV *Yap* shRNA-treated mice (Fig. 7B and C). These data suggested that these factors also contributed to fenofibrate-induced hepatomegaly when YAP was repressed. Additionally, YAP knockdown attenuated the induction of *Myc*, *Krt23*, and *Rhoa* by fenofibrate (Fig. 7A–C), indicating that YAP might be involved in the



induction of these genes by fenofibrate. We further detected the mRNA and protein expressions of these factors in fenofibrate-promoted liver regeneration. Similarly, fenofibrate treatment significantly upregulated the expression of MYC, KRT23, KRAS, and RHOA in mice post-PHx (Fig. 7D–F). These data suggested that in addition to YAP signaling, other factors, such as MYC, KRT23, RAS, and RHOA, might participate in the fenofibrate-induced hepatic proliferative response.

4. Discussion

Fenofibrate belongs to a category of drugs known as fibrates and has been used clinically as a lipid-regulating agent to treat patients with high cholesterol and high triglycerides²⁵. Accumulating evidence suggests that fenofibrate has clinical implications for treating liver diseases, including NAFLD, cholestasis, liver fibrosis, and drug-induced liver injury^{31,32,45,46}. Fenofibrate is reported to be a classical ligand of PPAR α ²⁶. In our most recent investigation, we discovered that the activation of PPAR α , prompted by WY-14643, stimulated hepatomegaly and liver regeneration *via* the YAP–TEAD pathway³⁴. The phenomenon of liver enlargement induced by fenofibrate has been observed, yet the underlying mechanism remains undisclosed. The current investigation revealed that fenofibrate promoted liver enlargement and regeneration, accompanied by hepatocellular hypertrophy near the CV area and increased hepatocellular proliferation surrounding the PV area, which was PPAR α -dependent and PPAR α expressed in hepatocytes played the dominant role in these processes. Mechanistically, fenofibrate activated YAP signaling by suppressing its K48-linked ubiquitination, promoting its K63-linked ubiquitination, and enhancing the interaction and transcriptional activity of the YAP–TEAD complex. Blocking the YAP–TEAD interaction or interfering with hepatic YAP expression markedly curtailed fenofibrate-triggered liver enlargement, which highlighted the pivotal role of the YAP pathway in fenofibrate-induced hepatomegaly. In addition to YAP, other factors, such as MYC, KRT23, RAS, and RHOA, were also associated with fenofibrate-induced liver enlargement and regeneration.

Clinically, fenofibrate is prescribed at doses of 150–300 mg/day for dyslipidaemia⁴⁵. It was also reported that the recommended dosage of fenofibrate to treat hypertriglyceridaemic patients is about 200–400 mg/day⁴⁷. According to the transition method based on body surface area, the equivalent dose in mice is approximately 20–60 mg/kg/day. Therefore, the low-dose (25 mg/kg/day) and medium-dose (50 mg/kg/day) groups in the current study are equivalent to the clinically effective doses. The dose of 50 mg/kg/day used in subsequent experiments aligns closely with this range, though it may be slightly higher than the clinically equivalent dosage. Fenofibrate is commonly prescribed for extended periods for treating severe hypertriglyceridemia and mixed dyslipidemia, with a

well-established safety profile and rare occurrences of severe side effects²⁵. In contrast, the potential utility of fenofibrate in promoting liver regeneration is more relevant in a short-term therapeutic context. Based on these considerations, fenofibrate would likely be safe and well-tolerated when used for liver regeneration post-PHx.

There have been reports of hepatomegaly in humans receiving fenofibrate in the EFFECT I trial (NCT02354976), which aimed to assess the impact of fenofibrate on liver fat among overweight or obese subjects with NAFLD and hypertriglyceridemia. The findings revealed a significant increase in both total liver volume and liver fat after fenofibrate treatment⁴⁸. Additionally, fenofibrate-induced hepatomegaly was observed in previous animal studies. Rodents exposed to PPAR α agonists, including fenofibrate, exhibited significant hepatomegaly, accompanied by peroxisome proliferation and increased fatty acid oxidation in the liver^{49,50}. Notably, the administration of fenofibrate has been reported to cause an increase in liver mass by approximately 50%–60% in rat models⁴⁹. Previous studies have indicated that fenofibrate induces hepatomegaly primarily through the stimulation of peroxisome proliferation and the upregulation of genes related to the cell cycle⁵¹. However, these studies did not fully address the specific signaling pathways that are implicated in the fenofibrate-induced hepatomegaly process. In the current study, we corroborate the findings of fenofibrate-induced hepatomegaly while introducing the YAP as a crucial mediator in this process, providing a deeper insight into the molecular mechanisms involved. Second, the current study extends beyond the previously established effects of fenofibrate on the liver, revealing the potential role of fenofibrate in promoting liver regeneration, a therapeutic implication not previously explored.

Fenofibrate, commonly prescribed for hyperlipidemia, exhibits significant effects beyond lipid regulation²⁵. It modulates hepatic glucose and bile acid homeostasis and affects oxidative stress and inflammation in the liver²⁶, highlighting its therapeutic potential in liver diseases. This drug has shown effectiveness in improving metabolic syndrome in NAFLD patients^{27,28} and offers an alternative treatment in chronic cholestatic liver disease cases unresponsive to UDCA^{29,30}. Additionally, fenofibrate's efficacy extends to treating liver fibrosis and drug-induced liver injury in animal models^{31,32}. However, whether fenofibrate treatment can promote PHx-induced liver regeneration remains unclear. Our results suggested that fenofibrate facilitates liver regeneration by regulating hepatocellular size and proliferative capacity. Liver transplantation and hepatic resection are typically the sole available means for treating end-stage liver diseases such as liver cancer, in which a sufficient liver size is necessary to ensure good postsurgical outcomes. When an undersized remnant liver cannot meet the functional demands, the patient might develop life-threatening postoperative complications such as small-for-size syndrome⁵². Our study showed that fenofibrate induced

Figure 4 Fenofibrate regulated the YAP signaling pathway. (A) Schematic diagram of the YAP signaling pathway. (B) mRNA expression of YAP downstream targets upon fenofibrate treatment in *Ppara*^{fl/fl} and *Ppara* ^{Δ Hep} mice ($n = 3$). (C) mRNA expression of YAP downstream targets upon fenofibrate treatment in *Ppara*^{fl/fl} and *Ppara* ^{Δ Hep} mice following PHx ($n = 3$). (D) Protein expression of YAP pathway components upon fenofibrate treatment in *Ppara*^{fl/fl} and *Ppara* ^{Δ Hep} mice. (E) Protein expression of YAP pathway components upon fenofibrate treatment in *Ppara*^{fl/fl} and *Ppara* ^{Δ Hep} mice following PHx. (F, G) Quantification of protein expression ($n = 3$). (H–J) HepG2 cell cultures underwent co-transfection using Flag-YAP alongside HA-Ub/HA-Ub-K48/HA-Ub-K63 plasmids, followed by fenofibrate treatment. Ubiquitination of YAP was identified through IP analysis. (K) Co-IP analysis between YAP and TEAD in HepG2 cells treated with either vehicle or fenofibrate. (L) Relative YAP–TEAD transcriptional activity was determined using luciferase assays ($n = 6$). Data are depicted as the mean \pm SD values; */**/****/***** indicates $P < 0.05/0.01/0.001/0.0001$, ns indicates not significant, *versus* the Control.

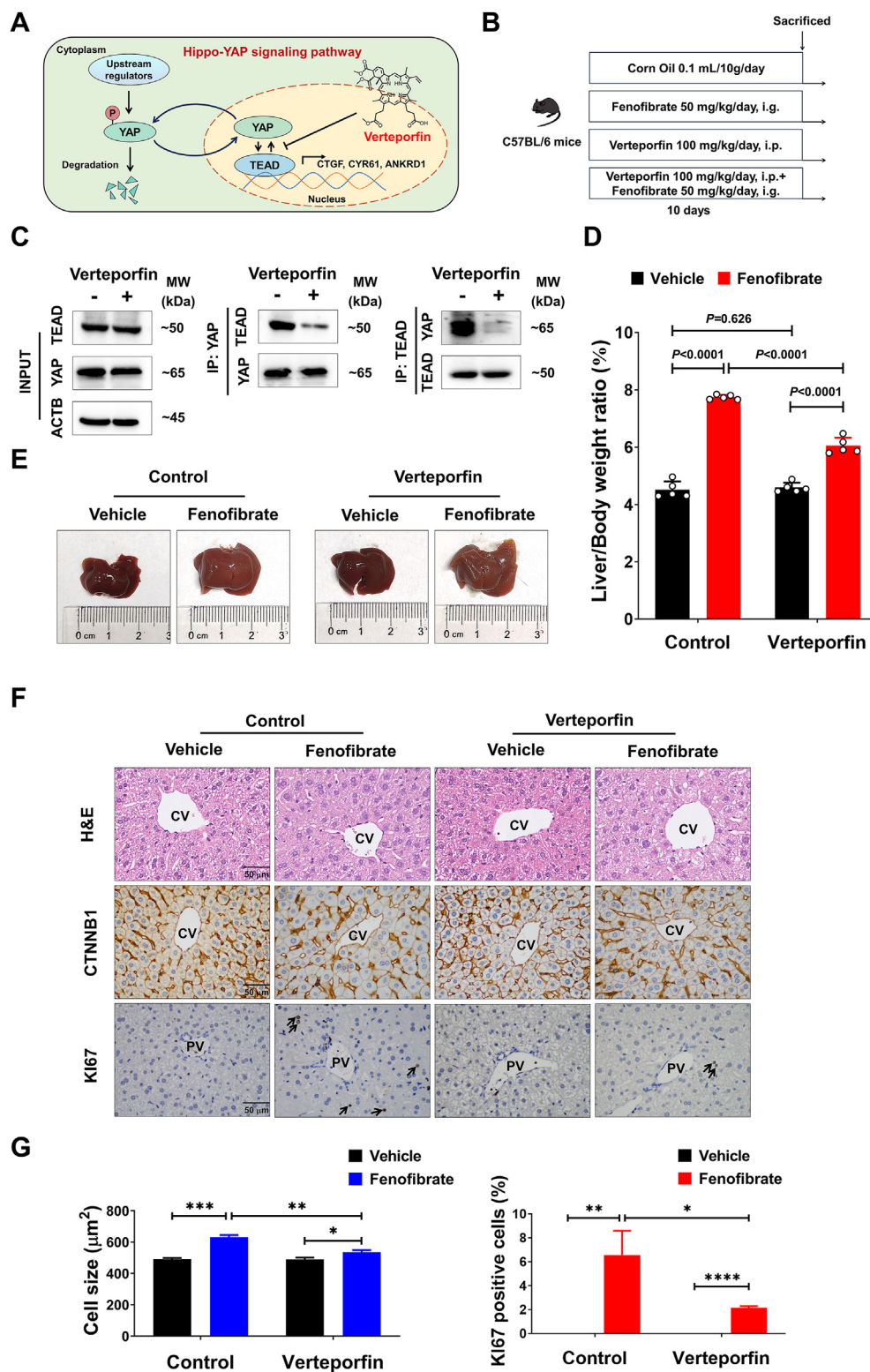


Figure 5 Inhibiting YAP–TEAD interaction attenuated fenofibrate-induced hepatomegaly. (A) Schematic diagram illustrating the inhibitory effect of verteporfin on the interaction between YAP and TEAD within the Hippo signaling cascade. (B) Experimental procedure in verteporfin-treated mice. (C) Co-IP analysis between YAP and TEAD in the liver of mice treated with either vehicle or verteporfin. (D) Ratios of liver weight to body weight ($n = 5$). (E) Representative photographs of mouse livers. (F) H&E, CTNNB1, and KI67 staining. (G) Quantitative analysis of cellular size and determination of KI67⁺ cell proportion ($n = 3$). Data are depicted as the mean \pm SD values; */**/**/* indicates $P < 0.05/0.01/0.001/0.0001$, versus the Control. Scale bar = 50 μm .

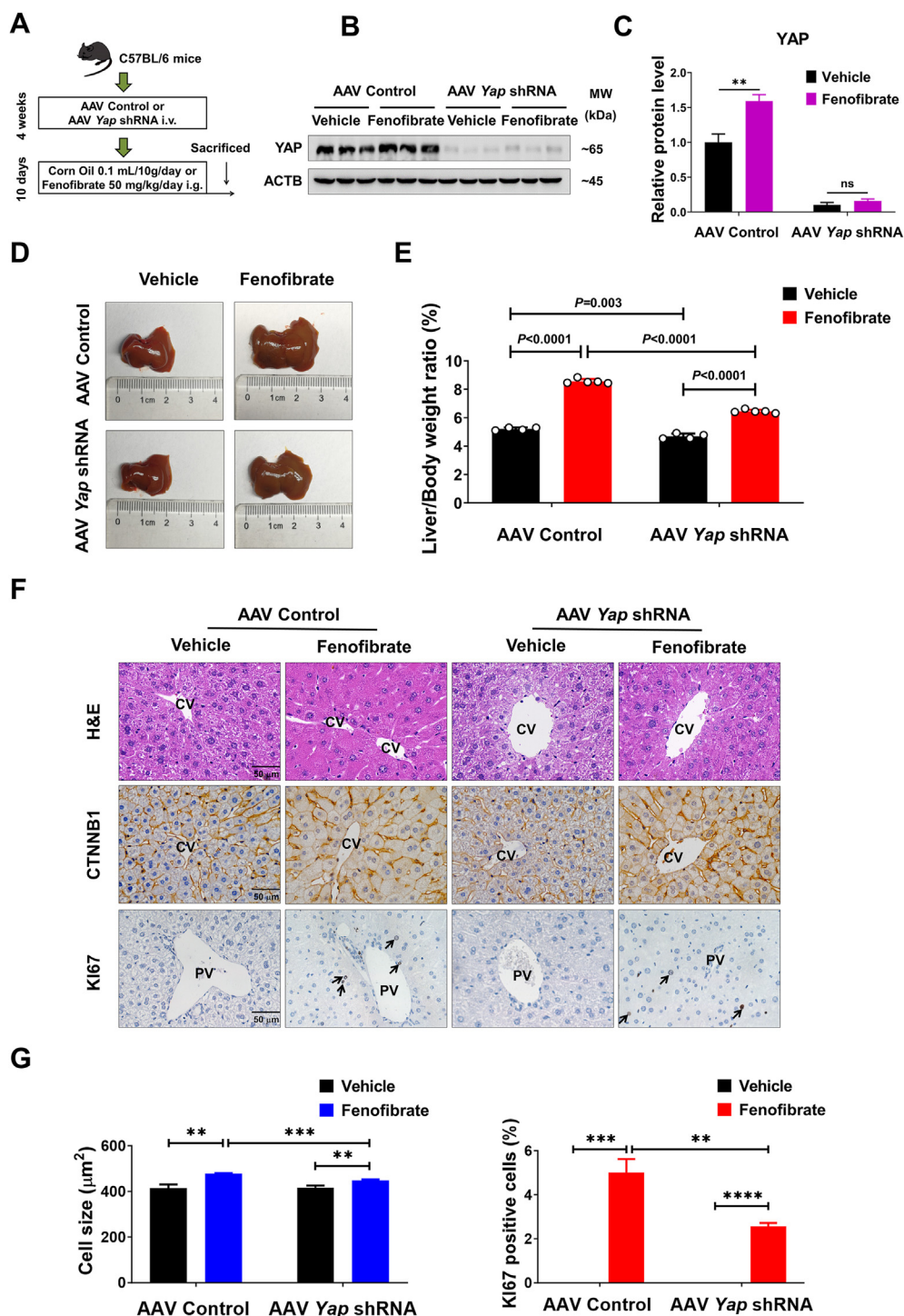


Figure 6 Hepatic YAP disruption suppressed fenofibrate-induced hepatomegaly. (A) Experimental procedure in AAV Control and AAV *Yap* shRNA mice. (B, C) Hepatic YAP protein level ($n = 3$). (D) Representative photographs of mouse livers. (E) Ratios of liver weight to body weight ($n = 4-5$). (F) H&E, CTNNB1, and Ki67 staining. (G) Quantitative analysis of cellular size and determination of Ki67⁺ cell proportion ($n = 3$). Data are depicted as the mean \pm SD values; **/***/**** indicates $P < 0.01/0.001/0.0001$, and ns indicates not significant, respectively, versus the Control. Scale bar = 50 μm .

hepatomegaly and accelerated liver weight recovery after PHx, indicating its pharmacological effect on maximizing the regenerative potential of undersized liver grafts and minimizing the risk of small-for-size syndrome following liver resection. These results suggested that fenofibrate is a promising medication for facilitating liver regeneration following PHx.

Fenofibrate was identified as an agonist of PPAR α , the critical regulator of lipid catabolism and energy balance in the liver. PPAR α is a transcription factor that can be activated by various ligands such as hypolipidemic drugs and experimental drug WY-14643⁵³. PPAR α activation induced by WY-14643 or fenofibrate has been reported to stimulate hepatocyte proliferation and

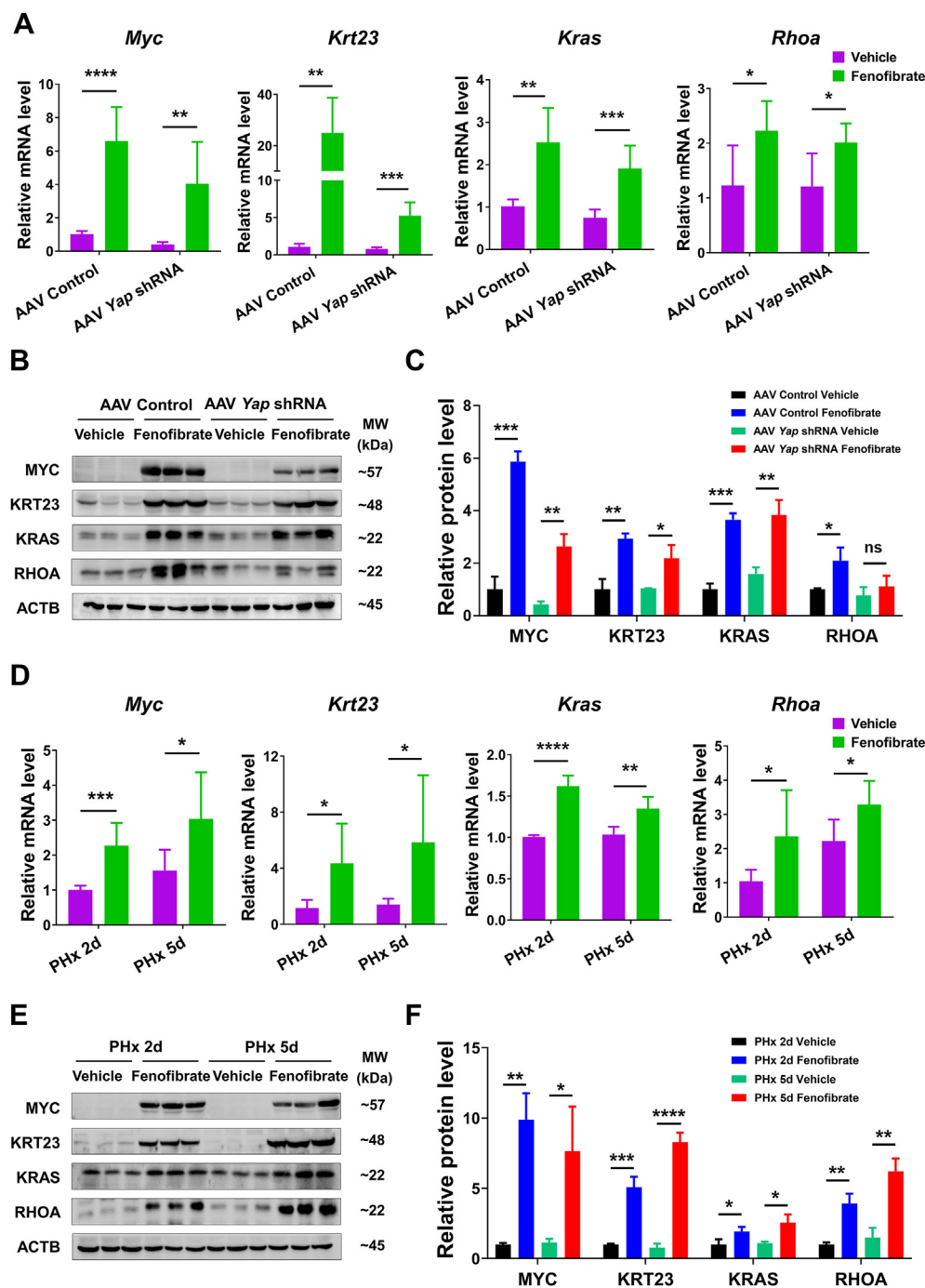


Figure 7 Other factors participated in fenofibrate-induced liver enlargement and regeneration. (A) mRNA levels of *Myc*, *Krt23*, *Kras*, and *Rhoa* in the *Yap* knockdown mouse model after fenofibrate treatment ($n = 3$). (B) Protein levels of MYC, KRT23, KRAS, and RHOA in the *Yap* knockdown mouse model after fenofibrate treatment. (C) Quantification of protein expression ($n = 3$). (D) mRNA levels of *Myc*, *Krt23*, *Kras*, and *Rhoa* in PHx mice after fenofibrate treatment ($n = 3$). (E) Protein levels of MYC, KRT23, KRAS, and RHOA in PHx mice after fenofibrate treatment. (F) Quantification of protein expression ($n = 3$). Data are depicted as the mean \pm SD values; */**/***/**** indicates $P < 0.05/0.01/0.001/0.0001$, ns indicates not significant, respectively, versus the Control.

result in hepatomegaly³³. In a dose-dependent manner, notable hepatomegaly was evident in all wild-type mice subjected to low, medium, and high dosages of fenofibrate, suggesting a potential dose–effect relationship between fenofibrate and liver enlargement. A species difference between humans and mice regarding PPAR α -induced liver enlargement has been reported, and PPAR α activation-induced hepatomegaly was found to be attenuated in

humans⁵⁴. PPAR α -humanized mice (hPPAR α mice) were also employed in our study, and the results showed that fenofibrate treatment also induced hepatomegaly in hPPAR α mice, while the impact was milder compared to wild-type mice (data not presented). PPAR α is expressed in various liver cell types, including hepatocytes, Kupffer cells, liver sinusoidal endothelial cells (LSECs), hepatic stellate cells (HSCs), and cholangiocytes.

Among these liver cell types, PPAR α is highly expressed in hepatocytes, with lower expression levels in non-parenchymal cells both in humans and mice⁵⁵. Previous studies have demonstrated that WY-14643-induced hepatic proliferative responses are mainly attributed to the activation of hepatocyte PPAR α relative to PPAR α expressed in non-parenchymal cells³⁷. Consistent with this finding, administration of fenofibrate increased the liver size and promoted liver regeneration in *Ppara*^{fl/fl} mice. However, these effects were absent in *Ppara* ^{Δ Hep} mice, indicating that hepatocyte PPAR α is essential in fenofibrate-induced liver enlargement and liver regeneration. Specifically, Gonzalez's group^{37,56} has demonstrated that Kupffer cell PPAR α primarily mediates the anti-inflammatory actions of PPAR α agonists, mainly through the suppression of pro-inflammatory cytokines like IL-15 and IL-18. Concerning LSECs, transcriptomic analyses revealed that PPAR α is transcribed in LSECs⁵⁷. However, the role of PPAR α in LSECs is less understood compared to that in hepatocytes. In HSCs, the expression of PPAR α was decreased when HSCs were activated⁵⁸. However, the exact role of PPAR α on HSC activation still needs to be confirmed. PPAR α agonist fenofibrate could inhibit LPS-induced pro-inflammatory cytokines such as TNF α and IL-6 in cholangiocytes⁵⁹. Interestingly, it was reported that PPAR α activation could enhance liver progenitor cell differentiation into hepatocytes⁶⁰. Overall, the role of PPAR α and the effects of fenofibrate on the different liver cell populations are still to be fully unveiled and can be considered as one of the future directions in the study of PPAR α in liver physiology.

YAP signaling is pivotal in governing liver growth and regeneration. YAP overexpression can trigger hepatic proliferative responses and induce liver overgrowth⁶¹. Deletion of the YAP upstream regulators MST1/2, which led to activation of YAP, induced significant hepatomegaly⁶². Additionally, YAP activity is critical to liver regeneration after PHx. A nuclear YAP accumulation was observed in the liver of rats post-PHx⁶³. Deletion of the *Yap* in mice impaired normal liver regeneration after PHx¹³. Pharmacological or genetic inhibition of the YAP upstream regulators MST1/2, which resulted in YAP activation, was found to facilitate liver regeneration following PHx^{12,15}. The current study indicated that YAP signaling was activated and that cell cycle-related proteins were upregulated upon fenofibrate treatment, indicating that YAP activation is an essential mechanism in fenofibrate-promoted hepatomegaly and liver regeneration. Post-translational modifications (PTMs) exert regulatory effects on the transcriptional activity of YAP. Here, we found that fenofibrate treatment increased K63-linked YAP polyubiquitination and decreased K48-linked YAP polyubiquitination, consistent with the findings of elevated YAP protein levels and augmented YAP-TEAD transcriptional activity. However, YAP activity is also regulated by other PTMs, such as SUMOylation, methylation, acetylation, and *O*-GlcNAcylation⁶⁴. Future investigations are needed to determine whether fenofibrate regulates other PTMs of YAP. Moreover, fenofibrate enhanced the binding and transcriptional activity of YAP-TEAD. Further *in vivo* studies using YAP-TEAD inhibitor verteporfin validated the involvement of the YAP-TEAD complex in fenofibrate-induced hepatomegaly. A model of liver-specific *Yap* disruption was established by AAV *Yap* shRNA treatment in mice. Suppression of YAP expression diminished the upregulation of CTGF, CYR61, and ANKRD1 upon fenofibrate administration. However, CCNA1 still showed obvious upregulation after fenofibrate administration in AAV *Yap* shRNA mice, suggesting that the induction of fenofibrate on

specific cell cycle-related proteins was maintained when YAP was suppressed. Other factors, in addition to YAP, might participate in fenofibrate-induced hepatomegaly. These findings substantiate the vital contribution of YAP in the processes of fenofibrate-triggered liver enlargement and regeneration.

Many signaling pathways have been found to regulate and be critical for hepatomegaly and liver regeneration induced by PPAR α activation. MYC was found to be associated with the PPAR α activation-induced hepatocellular proliferative response. The knockout of *Myc* in mouse hepatocytes attenuated the hepatic proliferative response induced by PPAR α agonist WY-14643⁴³. KRT23, whose expression is amplified in the presence of MYC, regulates hepatocyte growth and proliferation during the PPAR α -induced hepatic proliferative response⁴². Additionally, it has been reported that deficiency of PPAR α hampered the normal progression of liver regeneration, which was closely associated with impaired activation of RAS and RHOA⁴⁴. Therefore, we hypothesized that MYC, KRT23, RAS, and RHOA might contribute to the hepatomegaly and liver regeneration induced by fenofibrate. In our study, while the knockdown of *Yap* or pharmacological inhibition of YAP-TEAD partially mitigated fenofibrate-induced hepatomegaly, it did not entirely prevent it. This led us to speculate the involvement of additional factors in this process. Hence, we further investigated the mRNA and protein expression of *Myc*, *Krt23*, *Kras*, and *Rhoa*. In the current study, although the induction of MYC and KRT23 was repressed when *Yap* was knocked down, a significant upregulation of MYC and KRT23 by fenofibrate was observed even after YAP was disrupted. We assumed that induction of these two factors participated in fenofibrate-induced hepatomegaly when YAP was repressed. The expression of *Kras* was still increased in AAV *Yap* shRNA mice after fenofibrate treatment. The activation of RAS might upregulate CCNA1 upon fenofibrate treatment in the *Yap* knockdown mouse model. Similarly, the induction effects of *Myc*, *Krt23*, *Kras*, and *Rhoa* were also observed in fenofibrate-treated mice post-PHx, suggesting these factors might also participate in fenofibrate-accelerated liver regeneration. In addition to YAP, other factors, such as MYC, KRT23, RAS, and RHOA, participate in fenofibrate-induced liver enlargement and regeneration.

Interestingly, hepatocellular hypertrophy and proliferation induced by fenofibrate showed a clear zonal difference: augmented hepatocyte proliferation was noted adjacent to the PV area, while increased hepatocyte size was observed around the CV zone. Previous studies have shown that the induction of hepatic enzymes is related to hepatocellular hypertrophy⁶⁵. CYP4A, a well-characterized PPAR α target, showed higher expression in the CV area. Induction of CYP4A by peroxisome proliferators was previously found to be largely restricted to hepatocytes around the CV area⁶⁶. A different zonal heterogeneity in hepatocytes induced by fibrate drugs was also reported; specifically, the upregulation of β -oxidation-related enzymes and peroxisome proliferation was more pronounced in hepatocytes neighboring the CV area compared to those surrounding the PV zone⁶⁷. Localization of YAP in the nucleus was predominantly noted in cholangiocytes and hepatocytes adjacent to the PV area, whereas hepatocytes neighboring the CV area exhibited minimal nuclear YAP presence⁹. Previous studies showed that YAP overexpression specifically induced the proliferation of periportal hepatocytes⁶⁸. Thus, we assumed that the enhanced proliferation of hepatocytes in the PV zone might be attributed to YAP activation induced by fenofibrate.

5. Conclusions

The current investigation illustrates that fenofibrate triggers hepatomegaly and stimulates liver regeneration post-PHx, concomitant with hepatocellular enlargement bordering the CV zone and hepatocyte proliferation neighboring the PV zone, which is PPAR α -dependent and PPAR α expressed in hepatocytes plays the dominant role in these processes. Fenofibrate activates YAP signaling by suppressing K48-linked ubiquitination of YAP, promoting K63-linked ubiquitination of YAP, and enhancing the interaction and transcriptional activity of the YAP–TEAD. Inhibition of YAP–TEAD interaction or suppression of hepatic YAP expression significantly represses fenofibrate-induced hepatomegaly, indicating that YAP signaling is critical for this process. Other factors, such as MYC, KRT23, RHOA, and RAS, also contribute to the hepatic proliferative responses induced by fenofibrate. These results highlight the essential role of YAP in fenofibrate-induced hepatomegaly and -accelerated liver regeneration. These findings offer novel insights for the potential use of fenofibrate as a medication for promoting liver regeneration after PHx.

Acknowledgments

The work was supported by the National Key R&D Program of China (2022YFA1104900 to Huichang Bi, 2022YFA1106700 to Xiao Yang), the National Natural Science Foundation of China (grants 82025034 and U23A20535 to Huichang Bi, grants 82304603 to Shicheng Fan), the Shenzhen Science and Technology Program (No. KQTD20190929174023858 to Huichang Bi, China), the Science and Technology Innovation Project of Guangdong Medical Products Administration (2023ZDZ06 to Huichang Bi, China), the National Postdoctoral Program for Innovative Talents (BX20230151 to Shicheng Fan, China), the China Postdoctoral Science Foundation (2023M731570 to Shicheng Fan), the Guangdong Basic and Applied Basic Research Foundation (2023A1515012859 to Shicheng Fan, China), the Guangdong Medical Research Foundation (A2023109 to Shicheng Fan, China). Cartoons in graphic abstract were created with BioRender.com (Agreement number: NM26IJZBON).

Author contributions

Shicheng Fan: Conceptualization, Methodology, Validation, Formal analysis, Investigation, Writing-Original Draft, Writing-Review & Editing, Funding acquisition. Yue Gao: Methodology, Validation, Formal analysis, Investigation, Writing-Review & Editing. Pengfei Zhao: Methodology, Validation, Investigation. Guomin Xie, Methodology, Investigation. Yanying Zhou: Methodology, Investigation. Xiao Yang: Funding acquisition. Xuan Li: Investigation. Shuaishuai Zhang: Methodology. Frank J. Gonzalez: Conceptualization, Methodology. Aijuan Qu: Methodology, Resources. Min Huang: Conceptualization, Resources. Huichang Bi: Conceptualization, Methodology, Resources, Writing-Review & Editing, Supervision, Project administration, Funding acquisition.

Conflicts of interest

The authors declare no conflicts of interest.

Appendix A. Supporting information

Supporting information to this article can be found online at <https://doi.org/10.1016/j.apsb.2024.03.030>.

References

- Petrowsky H, Fritsch R, Guckenberger M, De Oliveira ML, Dutkowski P, Clavien PA. Modern therapeutic approaches for the treatment of malignant liver tumours. *Nat Rev Gastroenterol Hepatol* 2020;**17**:755–72.
- Michalopoulos GK, Bhushan B. Liver regeneration: biological and pathological mechanisms and implications. *Nat Rev Gastroenterol Hepatol* 2021;**18**:40–55.
- Miyaoka Y, Ebato K, Kato H, Arakawa S, Shimizu S, Miyajima A. Hypertrophy and unconventional cell division of hepatocytes underlie liver regeneration. *Curr Biol* 2012;**22**:1166–75.
- Clavien P, Petrowsky H, DeOliveira ML, Graf R. Medical progress: strategies for safer liver surgery and partial liver transplantation. *N Engl J Med* 2007;**356**:1545–59.
- Sandstrom P, Rosok BI, Sparrelid E, Larsen PN, Larsson AL, Lindell G, et al. ALPPS improves resectability compared with conventional two-stage hepatectomy in patients with advanced colorectal liver metastasis results from a Scandinavian multicenter randomized controlled trial (LIGRO Trial). *Ann Surg* 2018;**267**:833–40.
- Fausto N, Campbell JS, Riehle KJ. Liver regeneration. *Hepatology* 2006;**43**:S45–53.
- Michalopoulos GK. Liver regeneration after partial hepatectomy critical analysis of mechanistic dilemmas. *Am J Pathol* 2010;**176**:2–13.
- Forbes SJ, Newsome PN. Liver regeneration—mechanisms and models to clinical application. *Nat Rev Gastroenterol Hepatol* 2016;**13**:473–85.
- Patel SH, Camargo FD, Yimlamai D. Hippo signaling in the liver regulates organ size, cell fate, and carcinogenesis. *Gastroenterology* 2017;**152**:533–45.
- Camargo FD, Gokhale S, Johnnidis JB, Fu D, Bell GW, Jaenisch R, et al. YAP1 increases organ size and expands undifferentiated progenitor cells. *Curr Biol* 2007;**17**:2054–60.
- Mugahid D, Kalocsay M, Liu X, Gruver JS, Peshkin L, Kirschner MW. YAP regulates cell size and growth dynamics via non-cell autonomous mediators. *Elife* 2020;**9**:e53404.
- Loforese G, Malinka T, Keogh A, Baier F, Simillion C, Montani M, et al. Impaired liver regeneration in aged mice can be rescued by silencing Hippo core kinases MST1 and MST2. *EMBO Mol Med* 2017;**9**:46–60.
- Oh SH, Swiderska-Syn M, Jewell ML, Premont RT, Diehl AM. Liver regeneration requires Yap1–TGF β -dependent epithelial–mesenchymal transition in hepatocytes. *J Hepatol* 2018;**69**:359–67.
- Zhang Y, Desai A, Yang SY, Bae KB, Antczak MI, Fink SP, et al. Inhibition of the prostaglandin-degrading enzyme 15-PGDH potentiates tissue regeneration. *Science* 2015;**348**:aaa2340.
- Fan F, He Z, Kong LL, Chen Q, Yuan Q, Zhang S, et al. Pharmacological targeting of kinases MST1 and MST2 augments tissue repair and regeneration. *Sci Transl Med* 2016;**8**:352ra108.
- Chan BKY, Elmasry M, Forootan SS, Russomanno G, Bunday TM, Zhang F, et al. Pharmacological activation of Nrf2 enhances functional liver regeneration. *Hepatology* 2021;**74**:973–86.
- Gao Y, Fan S, Li H, Jiang Y, Yao X, Zhu S, et al. Constitutive androstane receptor induced-hepatomegaly and liver regeneration is partially via yes-associated protein activation. *Acta Pharm Sin B* 2021;**11**:727–37.
- Tschor C, Kachaylo E, Limani P, Raptis DA, Linecker M, Tian Y, et al. Constitutive androstane receptor (Car)-driven regeneration protects liver from failure following tissue loss. *J Hepatol* 2016;**65**:66–74.
- Jiang Y, Feng D, Ma X, Fan S, Gao Y, Fu K, et al. Pregnane X receptor regulates liver size and liver cell fate by yes-associated protein activation in mice. *Hepatology* 2019;**69**:343–58.
- Zhao YY, Yao XP, Jiao TY, Tian JN, Gao Y, Fan SC, et al. Schisandrol B promotes liver enlargement via activation of PXR and YAP pathways in mice. *Phytomedicine* 2021;**84**:153520.
- Kawaguchi T, Kodama T, Hikita H, Tanaka S, Shigekawa M, Nawa T, et al. Carbamazepine promotes liver regeneration and survival in mice. *J Hepatol* 2013;**59**:1239–45.

22. Lv M, Zeng H, He Y, Zhang J, Tan G. Dexmedetomidine promotes liver regeneration in mice after 70% partial hepatectomy by suppressing NLRP3 inflammasome not TLR4/NF κ B. *Int Immunopharm* 2018;**54**:46–51.
23. Jiao T, Yao X, Zhao Y, Zhou Y, Gao Y, Fan S, et al. Dexamethasone-induced liver enlargement is related to PXR/YAP activation and lipid accumulation but not hepatocyte proliferation. *Drug Metab Dispos* 2020;**48**:830–9.
24. Yao XP, Jiao TY, Jiang YM, Fan SC, Zhao YY, Yang X, et al. PXR mediates mifepristone-induced hepatomegaly in mice. *Acta Pharmacol Sin* 2022;**43**:146–56.
25. McKeage K, Keating GM. Fenofibrate: a review of its use in dyslipidaemia. *Drugs* 2011;**71**:1917–46.
26. Ghonem NS, Assis DN, Boyer JL. Fibrates and cholestasis. *Hepatology* 2015;**62**:635–43.
27. Lawitz EJ, Bhandari BR, Ruane PJ, Kohli A, Harting E, Ding D, et al. Fenofibrate mitigates hypertriglyceridemia in nonalcoholic steatohepatitis patients treated with cilofexor/firsocostat. *Clin Gastroenterol Hepatol* 2023;**21**:143–52.
28. El-Haggag SM, Mostafa TM. Comparative clinical study between the effect of fenofibrate alone and its combination with pentoxifylline on biochemical parameters and liver stiffness in patients with non-alcoholic fatty liver disease. *Hepatol Int* 2015;**9**:471–9.
29. Cheung AC, Lapointe-Shaw L, Kowgier M, Meza-Cardona J, Hirschfield GM, Janssen HL, et al. Combined ursodeoxycholic acid (UDCA) and fenofibrate in primary biliary cholangitis patients with incomplete UDCA response may improve outcomes. *Aliment Pharmacol Ther* 2016;**43**:283–93.
30. Levy C, Peter JA, Nelson DR, Keach J, Petz J, Cabrera R, et al. Pilot study: fenofibrate for patients with primary biliary cirrhosis and an incomplete response to ursodeoxycholic acid. *Aliment Pharmacol Ther* 2011;**33**:235–42.
31. Rodriguez-Vilarrupla A, Lavina B, Garcia-Caldero H, Russo L, Rosado E, Roglans N, et al. PPAR α activation improves endothelial dysfunction and reduces fibrosis and portal pressure in cirrhotic rats. *J Hepatol* 2012;**56**:1033–9.
32. Zhang Y, Pan YY, Xiong RR, Zheng JJ, Li QY, Zhang SS, et al. FGF21 mediates the protective effect of fenofibrate against acetaminophen-induced hepatotoxicity via activating autophagy in mice. *Biochem Biophys Res Commun* 2018;**503**:474–81.
33. Harmon GS, Lam MT, Glass CK. PPARs and lipid ligands in inflammation and metabolism. *Chem Rev* 2011;**111**:6321–40.
34. Fan S, Gao Y, Qu A, Jiang Y, Li H, Xie G, et al. YAP–TEAD mediates PPAR α -induced hepatomegaly and liver regeneration in mice. *Hepatology* 2022;**75**:74–88.
35. Song D, Luo M, Dai M, Bu S, Wang W, Zhang B, et al. PPAR α -dependent increase of mouse urine output by gemfibrozil and fenofibrate. *Can J Physiol Pharmacol* 2017;**95**:199–205.
36. Toda K, Okada T, Miyaoura C, Saibara T. Fenofibrate, a ligand for PPAR α , inhibits aromatase cytochrome P450 expression in the ovary of mouse. *J Lipid Res* 2003;**44**:265–70.
37. Brocker CN, Yue J, Kim D, Qu A, Bonzo JA, Gonzalez FJ. Hepatocyte-specific PPARA expression exclusively promotes agonist-induced cell proliferation without influence from nonparenchymal cells. *Am J Physiol Gastrointest Liver Physiol* 2017;**312**:G283–99.
38. Deng L, Meng T, Chen L, Wei W, Wang P. The role of ubiquitination in tumorigenesis and targeted drug discovery. *Signal Transduct Targeted Ther* 2020;**5**:11.
39. Liu M, Yan M, Lv H, Wang B, Lv X, Zhang H, et al. Macrophage K63-linked ubiquitination of YAP promotes its nuclear localization and exacerbates atherosclerosis. *Cell Rep* 2020;**32**:107990.
40. Yao F, Zhou Z, Kim J, Hang Q, Xiao Z, Ton BN, et al. SKP2- and OTUD1-regulated non-proteolytic ubiquitination of YAP promotes YAP nuclear localization and activity. *Nat Commun* 2018;**9**:2269.
41. Russell JO, Camargo FD. Hippo signalling in the liver: role in development, regeneration and disease. *Nat Rev Gastroenterol Hepatol* 2022;**19**:297–312.
42. Kim D, Brocker CN, Takahashi S, Yagai T, Kim T, Xie GM, et al. Keratin 23 is a peroxisome proliferator-activated receptor alpha-dependent, MYC-amplified oncogene that promotes hepatocyte proliferation. *Hepatology* 2019;**70**:154–67.
43. Qu AJ, Jiang CT, Cai Y, Kim JH, Tanaka N, Ward JM, et al. Role of Myc in hepatocellular proliferation and hepatocarcinogenesis. *J Hepatol* 2014;**60**:331–8.
44. Wheeler MD, Smutney OM, Check JF, Rusyn I, Schulte-Hermann R, Thurman RG. Impaired Ras membrane association and activation in PPAR α knockout mice after partial hepatectomy. *Am J Physiol Gastrointest Liver Physiol* 2003;**284**:302–12.
45. Dai MY, Yang JL, Xie MZ, Lin J, Luo M, Hua HY, et al. Inhibition of JNK signalling mediates PPAR-dependent protection against intrahepatic cholestasis by fenofibrate. *Br J Pharmacol* 2017;**174**:3000–17.
46. Fernandez-Miranda C, Perez-Carreras M, Colina F, Lopez-Alonso G, Vargas C, Solis-Herruzo JA. A pilot trial of fenofibrate for the treatment of non-alcoholic fatty liver disease. *Dig Liver Dis* 2008;**40**:200–5.
47. Balfour JA, McTavish D, Heel RC. Fenofibrate. A review of its pharmacodynamic and pharmacokinetic properties and therapeutic use in dyslipidaemia. *Drugs* 1990;**40**:260–90.
48. Oscarsson J, Onnerhag K, Riserus U, Sundén M, Johansson L, Jansson PA, et al. Effects of free omega-3 carboxylic acids and fenofibrate on liver fat content in patients with hypertriglyceridemia and non-alcoholic fatty liver disease: a double-blind, randomized, placebo-controlled study. *J Clin Lipidol* 2018;**12**:1390–403.
49. Gregus Z, Fekete T, Halaszi E, Gyurasics A, Klaassen CD. Effects of fibrates on the glycine conjugation of benzoic acid in rats. *Drug Metab Dispos* 1998;**26**:1082–8.
50. Park MK, Han Y, Kim MS, Seo E, Kang S, Park SY, et al. Reduction of food intake by fenofibrate is associated with cholecystokinin release in long-evans Tokushima rats. *Korean J Physiol Pharmacol* 2012;**16**:181–6.
51. Yang Q, Nagano T, Shah Y, Cheung C, Ito S, Gonzalez FJ. The PPAR α -humanized mouse: a model to investigate species differences in liver toxicity mediated by PPAR α . *Toxicol Sci* 2008;**101**:132–9.
52. Dahm F, Georgiev P, Clavien PA. Small-for-size syndrome after partial liver transplantation: definition, mechanisms of disease and clinical implications. *Am J Transplant* 2005;**5**:2605–10.
53. Bougarne N, Weyers B, Desmet SJ, Deckers J, Ray DW, Staels B, et al. Molecular actions of PPAR α in lipid metabolism and inflammation. *Endocr Rev* 2018;**39**:760–802.
54. Gonzalez FJ, Shah YM. PPAR α : mechanism of species differences and hepatocarcinogenesis of peroxisome proliferators. *Toxicology* 2008;**246**:2–8.
55. Berthier A, Johanns M, Zummo FP, Lefebvre P, Staels B. PPARs in liver physiology. *Biochim Biophys Acta, Mol Basis Dis* 2021;**1867**:166097.
56. Wang Y, Nakajima T, Gonzalez FJ, Tanaka N. PPARs as metabolic regulators in the liver: lessons from liver-specific PPAR-null mice. *Int J Mol Sci* 2020;**21**:2061.
57. Tegge AN, Rodrigues RR, Larkin AL, Vu L, Murali TM, Rajagopalan P. Transcriptomic analysis of hepatic cells in multicellular organotypic liver models. *Sci Rep* 2018;**8**:11306.
58. Han X, Wu Y, Yang Q, Cao G. Peroxisome proliferator-activated receptors in the pathogenesis and therapies of liver fibrosis. *Pharmacol Ther* 2021;**222**:107791.
59. Kempinska-Podhorodecka A, Abramczyk J, Cielica E, Hula B, Maciejowska H, Banales J, et al. Effect of low testosterone levels on the expression of proliferator-activated receptor alpha in female patients with primary biliary cholangitis. *Cells* 2023;**12**:2273.
60. Kim M, So J, Shin D. PPAR α activation promotes liver progenitor cell-mediated liver regeneration by suppressing YAP signaling in zebrafish. *Sci Rep* 2023;**13**:18312.

61. Dong JX, Feldmann G, Huang JB, Wu S, Zhang NL, Comerford SA, et al. Elucidation of a universal size-control mechanism in *Drosophila* and mammals. *Cell* 2007;**130**:1120–33.
62. Song H, Mak KK, Topol L, Yun KS, Hu JX, Garrett L, et al. Mammalian Mst1 and Mst2 kinases play essential roles in organ size control and tumor suppression. *Proc Natl Acad Sci U S A* 2010;**107**:1431–6.
63. Grijalva JL, Huizenga M, Mueller K, Rodriguez S, Brazzo J, Camargo F, et al. Dynamic alterations in Hippo signaling pathway and YAP activation during liver regeneration. *Am J Physiol Gastrointest Liver Physiol* 2014;**307**:196–204.
64. Yan F, Qian M, He Q, Zhu H, Yang B. The posttranslational modifications of Hippo–YAP pathway in cancer. *Biochim Biophys Acta Gen Subj* 2020;**1864**:129397.
65. Maronpot RR, Yoshizawa K, Nyska A, Harada T, Flake G, Mueller G, et al. Hepatic enzyme induction: histopathology. *Toxicol Pathol* 2010;**38**:776–95.
66. Lindros KO. Zonation of cytochrome P450 expression, drug metabolism and toxicity in liver. *Gen Pharmacol* 1997;**28**:191–6.
67. Lindauer M, Beier K, Volkl A, Fahimi HD. Zonal heterogeneity of peroxisomal enzymes in rat liver: differential induction by three divergent hypolipidemic drugs. *Hepatology* 1994;**20**:475–86.
68. Yimlamai D, Christodoulou C, Galli GG, Yanger K, Pepe-Mooney B, Gurung B, et al. Hippo pathway activity influences liver cell fate. *Cell* 2014;**157**:1324–38.